Water Supply

IWA PUBLISHING

Water Supply Vol 22 No 6, 5894 doi: 10.2166/ws.2022.216

Comparative study for assessing vulnerability to pollution in El Asnam plain, North of Algeria

Amina Rezig[a,b,*], Lucia Marinangeli[c] and Sofiane Saggai[a]

[a] Laboratoire de Génie de l'Eau et de l'Environnement en Milieu Saharien (GEEMS), Université KASDI Merbah, Ouargla 30 000, Algeria
[b] Institute of Technology, University of Bouira, Bouira 10 000, Algeria
[c] TELELAB – Remote Sensing and Planetology Laboratory, Department of Psychological, Health & Territorial Sciences (DISPUTer), Universita'Chieti-Pescara, Via Vestini, Chieti 31-66013, Italy
*Corresponding author. E-mail: amina22sba@yahoo.fr

ABSTRACT

Assessment of groundwater contamination is an efficient means to discover and carry out the demarcation of the more vulnerable zones to pollution from human activities. This study is focused on the plain of El Asnam (Northern Algeria) characterized by intensive agricultural activities. To protect the groundwater from pollution, it is necessary to determine vulnerable areas. This paper aims to generate groundwater vulnerability map using two models: DRASTIC and Susceptibility Index (SI) associated with the geographic information system (GIS) of El Asnam plain aquifer. The validation of these models to pollution was performed by comparing the nitrate distribution across the area with the classes of vulnerability and has proved that the SI model is the more valid one with 50% of the study area. Considering these results, the SI model may serve as an effective means to help the protection of groundwater and can eventually be used by decision makers and groundwater managers.

Key words: DRASTIC, El Asnam plain, GIS, groundwater vulnerability, nitrate, susceptibility index

HIGHLIGHTS

- Agricultural plain is vulnerable to contamination.
- Mapping of groundwater vulnerability indicate zones that have the most potential to contamination.
- Validation of results requires distribution of nitrate concentrations.
- The SI model serves as a tool for the protection of groundwater in agricultural plains.

GRAPHICAL ABSTRACT

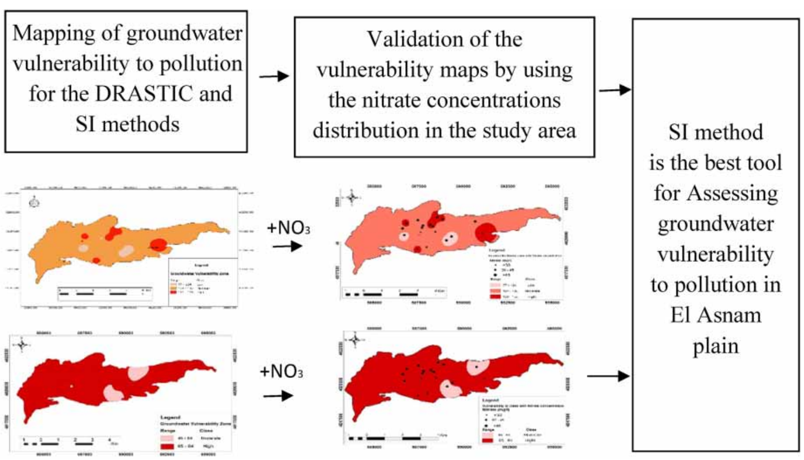

INTRODUCTION

Groundwater is considered as one of the pure sources of water, due to its low vulnerability to contamination (Jamrah *et al.* 2008). In this case, pollution is not easy to locate or to control and it may last years and sometimes centuries (Bhuvaneswaran & Ganesh 2019). Industrial, agricultural, and urban activities constitute potential origins of groundwater pollution and increase proportionally with high population growth and the expansion of urbanization (Rahman 2008). However, it is necessary to protect the groundwater from the threats of pollution mainly in areas with intense agricultural activities (Lake *et al.* 2003; Al Hallaq & Elaish 2012). In arid and semiarid areas, it is the principal origin of drinking water which makes its vulnerability assessment very important (Ghazavi & Ebrahimi 2015). It deals with the hydrogeological, pedological, and geological characteristics to demarcate zones with their vulnerability to groundwater contamination without taking into account the attenuation of pollutants to save the groundwater quality (Awawdeh *et al.* 2015). As a result, some zones are the most susceptible to pollution (Baalousha 2006; Al Hallaq & Elaish 2012). The evaluation of groundwater vulnerability requires many approaches that have been developed and most of them use index models that combine factors controlling the pollutants' movement between the ground surface and the saturated zone, thus giving vulnerability indices at various locations of soil (Magesh & Chandrasekar 2013; Sener & Davraz 2013; Al-Shatnawi *et al.* 2014; Kumar *et al.* 2014; Narmada *et al.* 2015; Nadiri *et al.* 2019; Amiri *et al.* 2020b).

One of the robust and widely model to evaluate the vulnerability of the groundwater to pollution is the DRASTIC method (Babiker *et al.* 2005; Shekhar & Pandey 2015), developed by Aller *et al.* (1987) for the U.S. Environmental Protection Agency (EPA) to characterize the pollution of groundwater (Aller *et al.* 1987; Zhang *et al.* 2010). This method supposes that the ground surface receives the contaminant and diffuses it by precipitation into the groundwater (Babiker *et al.* 2005), allowing it to have the water mobility (Aller *et al.* 1987). This method is based on seven physical and hydrogeological parameters allowing determination of the vulnerability to pollution for different locations, namely, depth to water table (D), net recharge (R), aquifer media (A), soil media (S), topography (T), the impact of vadose zone (I), and hydraulic conductivity (C) (Huan *et al.* 2012; Srinivasamoorthy *et al.* 2012; Neh *et al.* 2015; Shekhar & Pandey 2015; Khan & Jhariya 2019). This model adopts a two-tier ranking method: weight and rating, for obtaining the DRASTIC index at different locations and the vulnerability maps in a GIS environment (Sinan & Razack 2009).

Lately, several studies assessed the efficiency of the groundwater vulnerability by the use of the GIS environment and the DRASTIC model (Hrkal 2001; Babiker *et al.* 2005; Jamrah *et al.* 2008; Saidi *et al.* 2010; Al Hallaq & Elaish 2012; Huan *et al.* 2012; Iqbal *et al.* 2015; Zghibi *et al.* 2016; Ayed *et al.* 2017; Ahirwar & Shukla 2018; Machdar *et al.* 2018; Hasan *et al.* 2019; Mondal *et al.* 2019; Ncibi *et al.* 2020; Bera *et al.* 2021) and also, artificial intelligence models are used to evaluate the vulnerability (Nadiri *et al.* 2018).

The susceptibility index method (SI), created by Ribeiro in 2000, is a specific method for the evaluation of the agricultural susceptibility to pollution, caused mainly by nitrates (Ribeiro 2000). This model is based on 5 parameters: depth to water (D), net recharge (R), aquifer media (A), topography (T), and land use (LU), which is an influencing factor to evaluate agricultural pollution (van Beynen *et al.* 2012; Anane *et al.* 2013b). DRASTIC parameters here are used as a reference, except for the hydraulic conductivity, vadose zone, and the soil media. The first two parameters are ignored because of their low influence on pollution due to agricultural activities (Stigter *et al.* 2006). The last one is removed because it is already treated in the land use parameter (Francés *et al.* 2001; Anane *et al.* 2013a). The range of land use is based on CORINE Land-Cover ranking (Europea 1993), While the rest of the parameter ranges (D, R, A, T) are similar to the DRASTIC model (Ncibi *et al.* 2020).

The distribution of nitrate concentrations in the study area is utilized as an indicator of groundwater pollution, because the plain of El Asnam (Algeria) is characterized by its intense activities in agriculture and the overuse of pesticides.

This paper aims to evaluate the groundwater susceptibility of El Asnam plain (in northern Algeria) to pollution (Figure 1), which is primarily agricultural land with the widespread use of different types of pesticides and fertilizers. Finally, the comparison between the DRASTIC and SI models combined with GIS allows to determine which one is the most efficient for protecting and managing the groundwater system in this area.

MATERIALS AND METHODS

Study area

El Asnam plain is located in the department of Bouira in the central province of north Algeria with an area of 27.31 km^2 from latitude 36 °18′ N to 36° 20′ N and from longitude 3 °55′ E to 4 °03′ E (Figure 2). The altitude ranges between 470 and 560 m

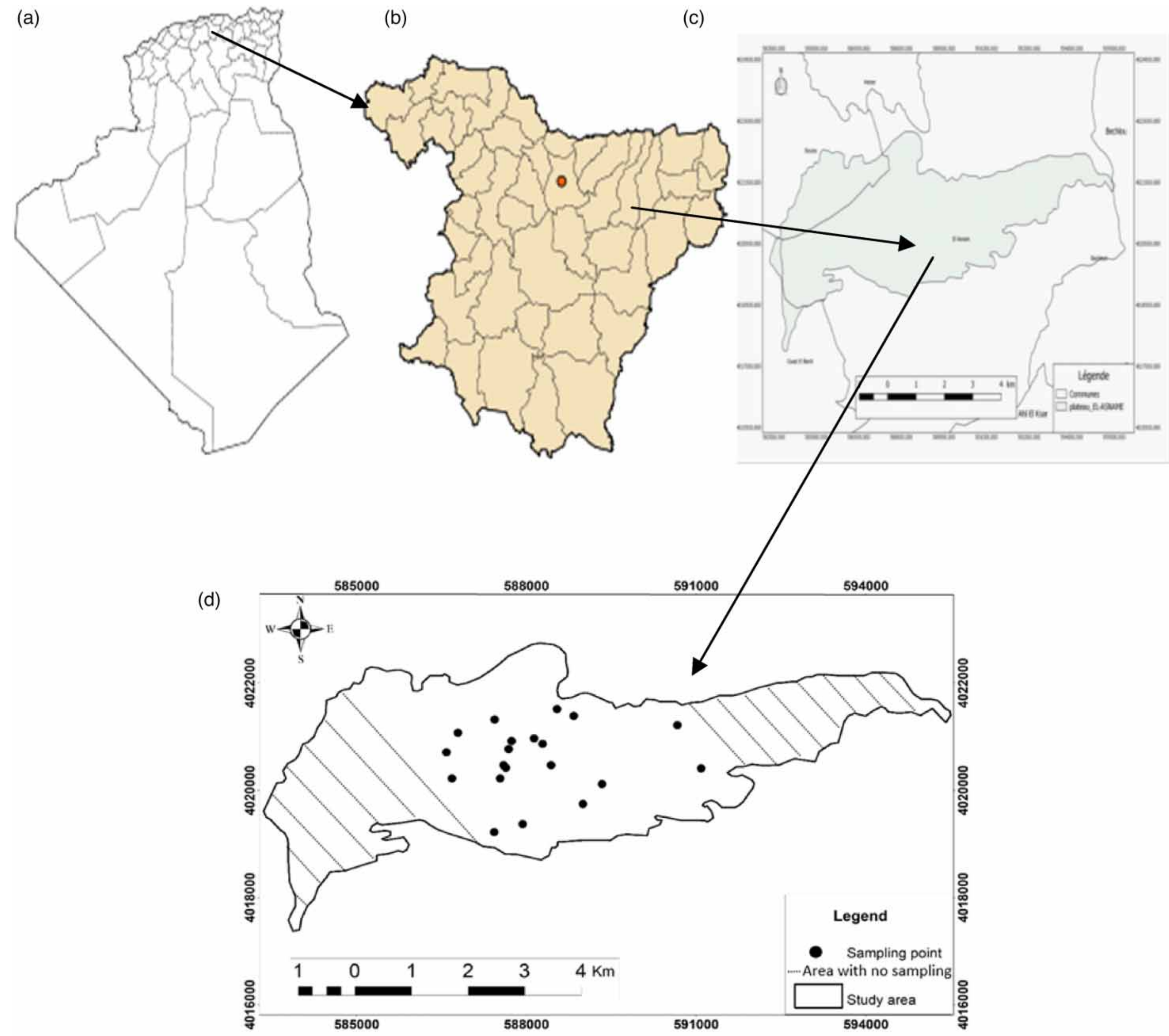

Figure 1 | (a) Algeria, (b) department of Bouira, (c) location of El Asnam plain, (d) sampling point location.

(Figure 3). This area covers fertile and gently-sloping soils encouraging farming activities, mainly cereals and vegetables, that have extended the contamination of groundwater in the plain (van Beynen *et al.* 2012). The region of Bouira has three sub-watersheds: Ed-Dous wadi, Zaiane wadi, and Sahel wadi grouped under the Sahel watershed, which belongs to the Soummam big watershed. This plain is located in the Soummam depression specifically in the western part that forms a junction between the northern hills and the southern hills. The surface hydrology appears mostly dense with a dendritic pattern (Figure 2) but the construction of the dam in 2003 and subsequent formation of the Tilesdit artificial basin changed the pattern of surface runoff. Furthermore, intensive agriculture almost completely canceled the surface streams at places.

The plain of El Asnam plain is bordered by the flysch sequence of Djurdjura Mountains to the north while more recent alluvial materials outcrop to the south. The geological setting (O.N.I.D. 1990) of the study area consists of a thick sequence of quaternary alluvium deposits (unit Qa-b in Figure 3), which cover an older (Miocene) conglomerate alternated to reddish clays succession (unit M in Figure 3). Unit M mostly consists of clay, silt, gravel, and sand (van Beynen *et al.* 2012).

From the perspective of climate, the plain is known for its dry and hot summer, cold and rainy winter. The average air temperature is 17.5 °C, while rainfall reaches 557.93 mm/year as estimated from 47 years' (1970–2017) rainfall data (Ribeiro 2000).

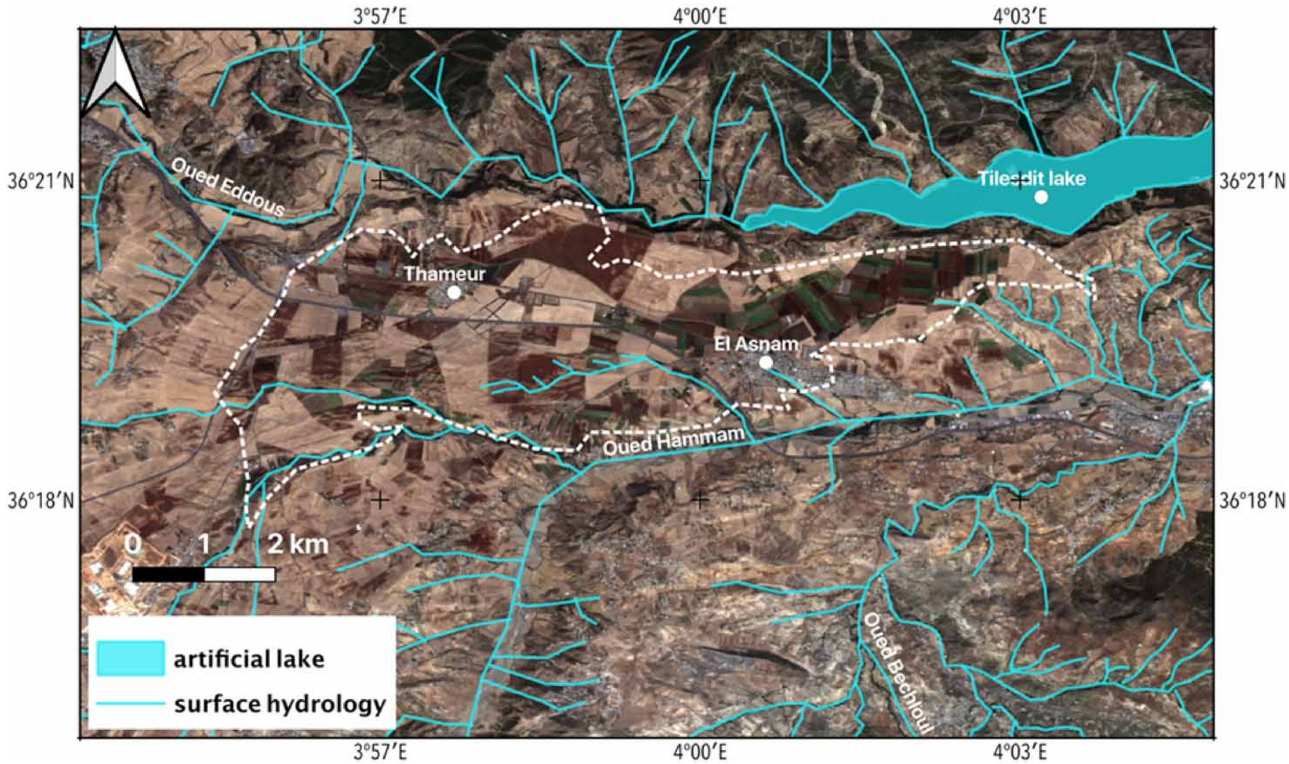

Figure 2 | Pan-sharpened LANDSAT8 image of the study area showing the intense agriculture from the rectangular pattern of the valley and the surface hydrology.

Methodology

The sustainability of the use of groundwater requires assessing their vulnerability to contamination. Mapping groundwater vulnerability to pollution is designed to indicate zones that have the most potential for contamination by applying the DRASTIC and the Susceptibility Index (SI) methods in GIS environment. Maps of these two models are based on weightage and rating, i.e. depth to water table (D), net recharge (R), aquifer media (A), soil media (S), topography (T), the impact of vadose zone (I), and hydraulic conductivity (C) for the DRASTIC model and depth to water (D), net recharge (R), aquifer media (A), topography (T), land use (LU) for the SI model. The mechanism of the models already mentioned requires seven steps: (1) the acquisition of data, (2) the production of maps for all parameters using a GIS environment, (3) the determination of the DRASTIC and SI indexes, (4) conception of the groundwater vulnerability maps, (5) identification of the vulnerability to pollution of the entire area, (6) application of nitrate distribution on the vulnerability maps, and (7) comparison between the methods to select the best one that offers efficient results.

DRASTIC model

The DRASTIC model is a standardized method for the assessment of groundwater vulnerability (Mallik *et al.* 2021). This model is one of the earliest used models, elaborated by the EPA for evaluating groundwater vulnerability in the United States (Aller *et al.* 1987). It is based on 7 parameters corresponding to 7 layers (Aller *et al.* 1987; Muhammad *et al.* 2015; Pacheco *et al.* 2015; Amiri *et al.* 2020a, 2020b; Ramakrishna *et al.* 2020; Boumaiza *et al.* 2021). A ranking system of ratings, weights, and ranges was designed using the 7 parameters to evaluate the hydrogeological setting and the index of the DRASTIC model (DI) of the plain (Table 1). The sum of the product of weights and ratings of all parameters gives this index as follow (Aller *et al.* 1987; Chitsazan & Akhtari 2009; Kadkhodaie *et al.* 2019; Sarkar & Pal 2021):

$$DI = DrDw + RrRw + ArAw + SrSw + TrTw + IrIw + CrCw \tag{1}$$

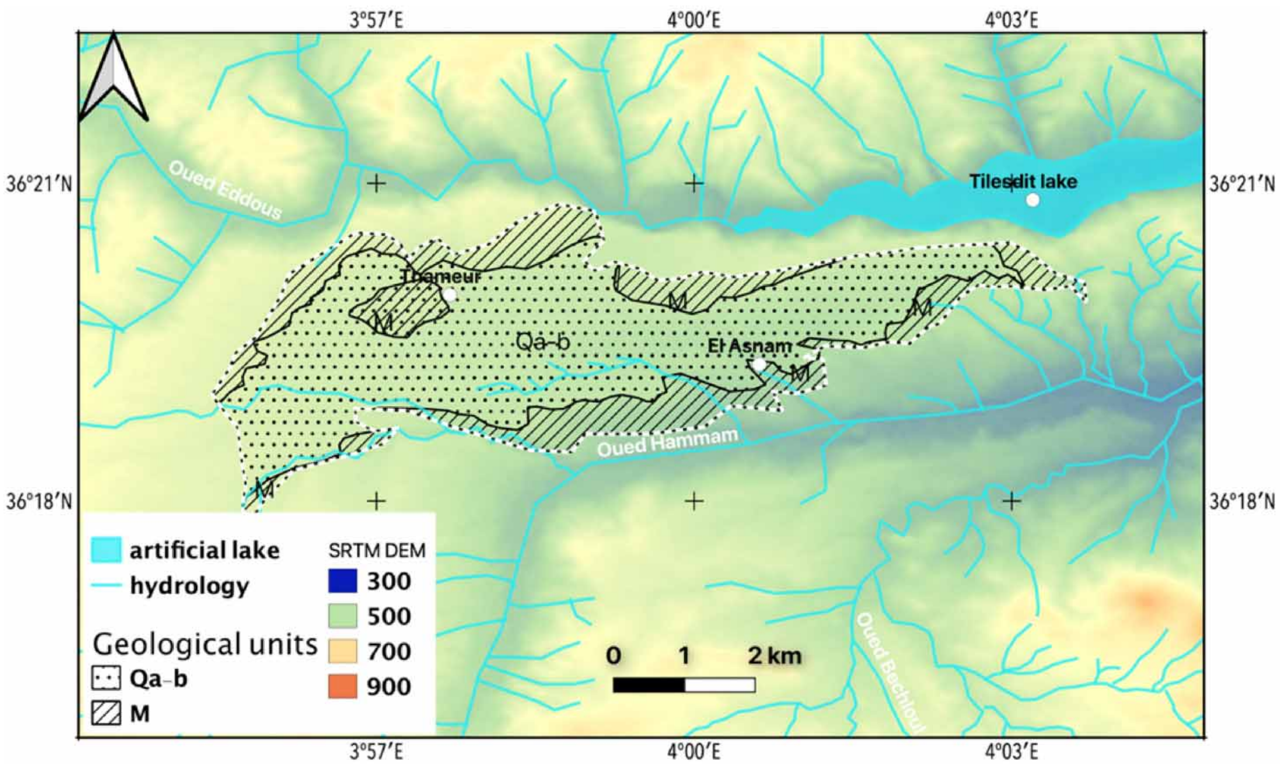

Figure 3 | Simplified geology over an SRTM DEM. The main river Oued Eddous and Hammam with the associated tributaries, border the study area.

where: D, R, A, S, T, I, and C are the 7 hydrogeological parameters, (r) is the rating, and (w) is the weight assigned for each parameter (Zhao & Pei 2012; Jilali *et al.* 2015; Jhariya *et al.* 2019). Determination of the DRASTIC index is useful to identify the susceptibility of zones to groundwater pollution relative to others (Teng *et al.* 2019; Barbulescu 2020). It represents qualitative risk vulnerability classes of very high, high, moderate, and low. A zone with a low DI is less vulnerable to pollution compared with the zones with moderate and high DI.

SI model

The SI was developed in Portugal by Ribeiro to assess the vertical groundwater susceptibility to diffuse agricultural pollution on a medium to large scale (1:50,000–1:200,000) (Ribeiro 2000). It is a modified version of the DRASTIC model, adapting a specific aspect by the inclusion of the parameter of land use, which introduces the influence of anthropogenic activities (Ribeiro *et al.* 2017; Pathak *et al.* 2021), and exclusion of the hydraulic conductivity (C), vadose zone (I), and soil media (S) parameters (Francés *et al.* 2001; Oroji & Karimi 2018). On the other hand, depth to the water table (D), net recharge (R), topography (T), and aquifer media (A) ratings in this method were multiplied by 10. Ratings and main classes of land use are presented in Table 2.

The equation for determining SI includes assigned weights to various parameters as follows:

$$SI = 0.186 \times D + 0.212 \times R + 0.259 \times A + 0.121 \times T + 0.222 \times LU \quad (2)$$

where: D, R, A, T, and LU are the 5 parameter ratings, 0.186, 0.212, 0.259, 0.121, and 0.222 are the weights assigned for each parameter (van Beynen *et al.* 2012). The final SI ranges from 0 to 100 because the ratings range also from 0 to 100 and it can be classified into 4 classes of vulnerability as difined in Table 3 (Ribeiro 2000; van Beynen *et al.* 2012; Anane *et al.* 2013b).

Table 1 | Range, rating, and weight of the DRASTIC parameters (Aller *et al.* 1987)

Depth to water (m)		Net recharge (mm)		Aquifer media		Soil media		Topography percent slope (%)		Impact of vadose zone		Hydraulic conductivity (m/s)	
Ranges	**Rating**	**Ranges**	**Rating**	**Ranges**	**Rating**	**Ranges**	**Rating**	**Ranges**	**Rating**	**Ranges**	**Rating**	**Ranges**	**Rating**
0–1.5	10	>255	9	Karst limestone	9–10	Thin or absent	10	0–2	10	Karst limsestone	8–10	$>9.4 \times 10^{-4}$	10
1.5–4.5	9	175–255	8	Basalt	2–10	Gravel		2–6	9	Basalt	2–10	4.7×10^{-4}–9.4×10^{-4}	8
4.5–9	7	100–175	6	Sand and gravel	4–9	Sand	9	6–12	5	Sand and gravel	6–9	32.9×10^{-5}–4.7×10^{-4}	6
9–15	5	50–100	3	Massive limestone	4–9	Peat	8	12–18	3	Metamorphic /igneous	2–8	14.7×10^{-5}–$32.9 \times 10 - ^{5}$	4
15–22	3	<50	1	Massive sandstone	4–9	Shrinking and/or aggregated clay	7	+18	1	Sand and gravel with significant, silt and clay	4–8	4.7×10^{-5}–14.7×10^{-5}	2
22–30	2	Weight	4	Shale sequences	5–9	Sandy loam	6	Weight	1	Bedded limestone, sandstone,shale		4.7×10^{-7}–4.7×10^{-5}	1
>30	1			Weathered metamorphic/ igneous	3–5	Loam	5			Sandstone		Weight	3
Weight	5			Thin bedded sandstone, limestone		Silty loam	4			Limestone	2–7		
				Metamorphic/ igneous	2–5	Clay loam	3			Shale	2–5		
				Massive shale	1–3	Muck	2			Silt/clay	1–2		
				Weight	3	Nonshrinking and nonaggregated clay	1			Weight	5		
						Weight	2						

Table 2 | Ratings of land use (Ribeiro 2000)

Land use categories	Rating
Industrial discharge, landfill, mines	100
Irrigated perimeters, paddy fields, irrigated perimeters, paddy fields, irrigated and non-irrigated annual cultures	90
Quarry, shipyard	80
Artificial covered zones, green zones, continuous urban zones	75
Permanent cultures (vines, orchards, olive trees, etc.)	70
Discontinuous urban zones	70
Pastures and agro-forest zones	50
Aquatic milieus (swamps, saline, etc.)	50
Forest and semi-natural zones	0

Table 3 | Vulnerability classes of the SI method (Ribeiro 2000)

Vulnerability class	Class
Low	<45
Moderate	45–64
High	65–84
Very high	85–100

RESULTS AND DISCUSSION OF DRASTIC AND SI METHODS

Depth to the water table (D)

Depth to water represents the distance between the ground surface and water table through which water infiltrates migrate in various materials before reach the aquifer (Aydi *et al.* 2013). Generally, the attenuation capacity of a contaminant decreases as the depth to water augments because deeper water tables induce longer infiltration times and vice versa (Aller *et al.* 1987). The weight of 5 was given to this parameter owing to its high potential in the assessment of vulnerability. The index of depth to water is a product of weight and rating (Dr x Dw) (Aller *et al.* 1987). The data of water table was obtained from 20 observation wells. It was found that groundwater levels (period 1970–2017) ranged from 9.7 m to 46.72 m (Figure 4) in the area. From Figure 4, the moderate value of depth to water is located in most parts of the plain. Four classes have determined i.e. 9–15, 15–22, 22–30, and >30 m, and assigned the ratings of 6, 5, 4, 3, 2, and 1. These values are presented as a grid to make it raster data for GIS function. Thus, interval range, weight, rating, resulting index, and area covered for the DRASTIC and SI models are given in Table 4. Areas with high groundwater tables have more chance of contamination because pollutants have short paths to move before reaching the water table, thus given a low rating. So, deeper groundwater shows a smaller rating value because it is less susceptible to pollution. The depth to water table map was rated based on DRASTIC and SI methods ratings.

Net recharge

It represents the quantity of water per unit area that infiltrates the land and reaches the groundwater. Net recharge represents an important factor for groundwater vulnerability because it is responsible for transporting pollutants between the surface and the aquifer. It is proportional to the susceptibility rating (Zghibi *et al.* 2016). The unit of net recharge is mm per year. The plain of El Asnam has a gentle slope. The main recharge source in the plain is precipitation. Net recharge is determined based on the annual rainfall data measured in a local climatology station from the period 1970 to 2017, hydrogeology, and geology of the plain. Net recharge found is 415 mm, according to the Williams and Kissel method (Williams & Kissel 1991), and assigned the rating of 9 (Figure 5) which is multiplied by 4 to get the DRASTIC index of the recharge in the plain (Table 5).

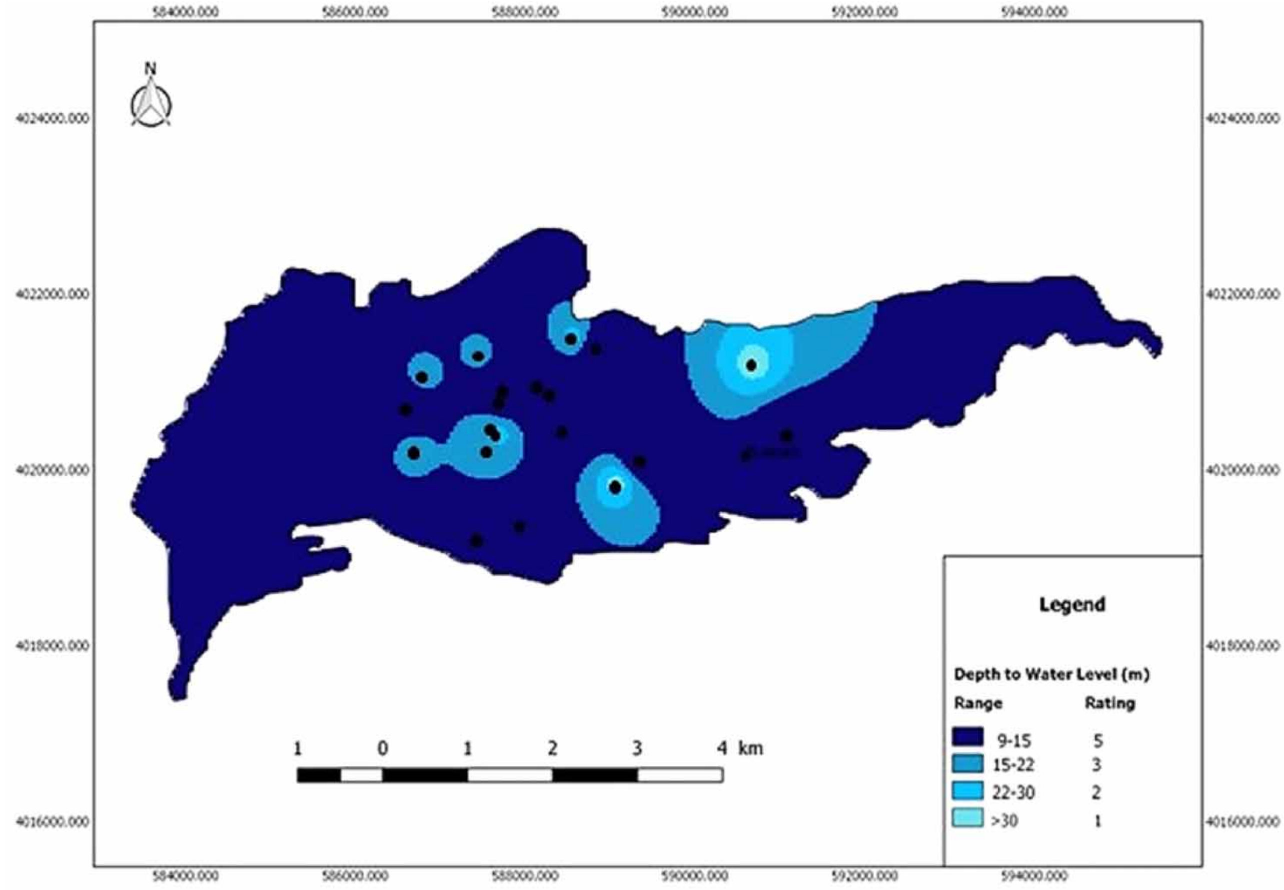

Figure 4 | Depth to water map of El Asnam plain (1970–2017).

Table 4 | Depth to water table range, rating, and index

Range (m)	Rating	Index DRASTIC (D_rD_w)	Index SI (D_rD_w)	Area(%)
9–15	5	25	9.3	86.27
15–22	3	15	5.58	10.71
22–30	2	10	3.72	2.47
>30	1	5	1.86	0.55

Aquifer media

It reflects the nature of the geological formation of the aquifer such as gravel and sand if it is alluvium or weathered zone and secondary porosities if it is hard rock (Abdeslam *et al.* 2017; Bhuvaneswaran & Ganesh 2019). The flow of an aquifer is affected by its media, which controls the pollutant's rate of contact with the aquifer (Al Hallaq & Elaish 2012; Saha & Alam 2014). Higher permeability and susceptibility of the aquifer are positively correlated with higher porosity and larger grain size within the aquifer (Anwar *et al.* 2002; Almasri 2008; Abdullahi 2009; Al Hallaq & Elaish 2012; Ahirwar & Shukla 2018; Venkatesan *et al.* 2019). In this study, the aquifer media (unconfined aquifer) has been extracted from subsurface geology, lithology map, and drilling profiles of the plain. The rating of the aquifer media varies between 4 for clay, 6 for the conglomerate, and 8 for gravel (Table 6). It shows the moderate susceptibility to pollution of the aquifer media (Figure 6). The weight corresponding to the aquifer media is 3.

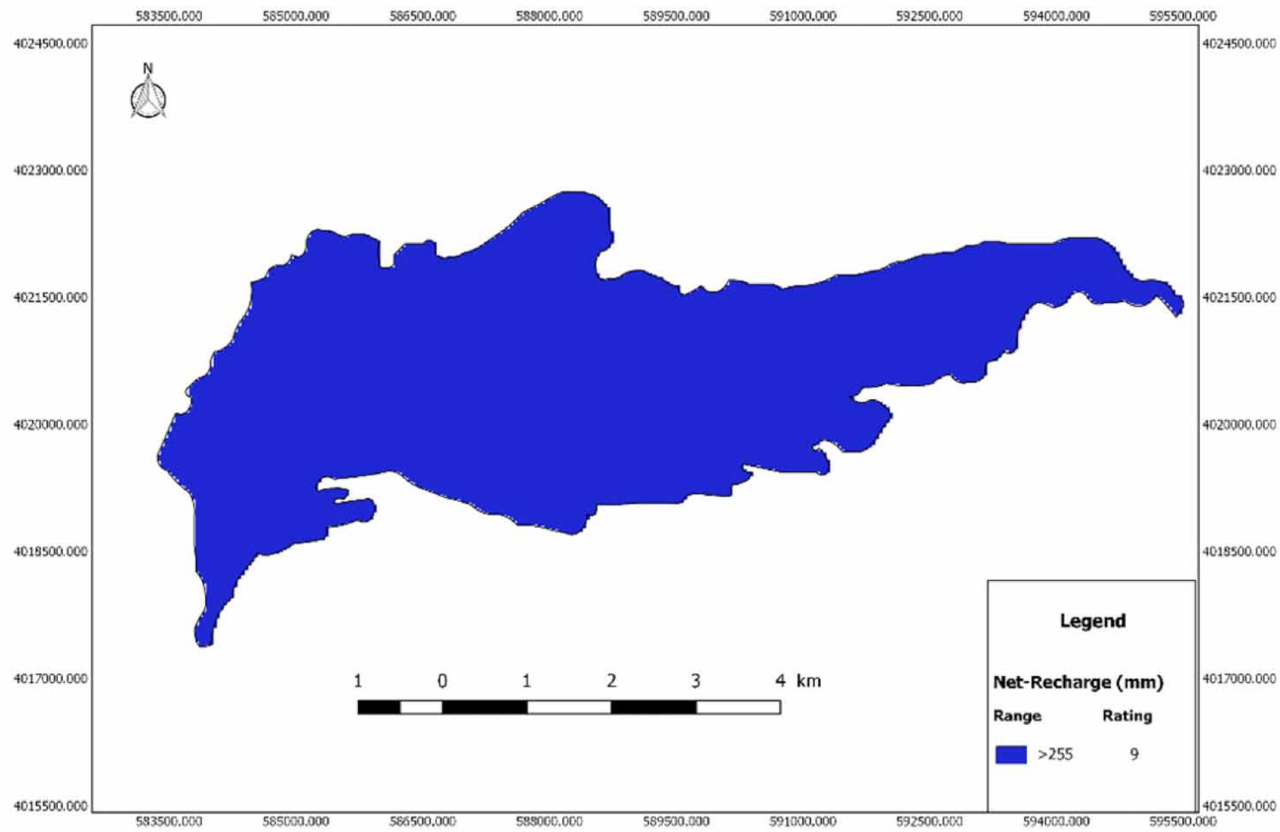

Figure 5 | Net recharge map of El Asnam plain (1970–2017).

Table 5 | Net recharge range, rating, and index

Range (mm)	**Rating**	**Index DRASIC (RrRw)**	**Index SI (RrRw)**	**Area(%)**
>255	9	36	19.08	100

Table 6 | Aquifer media range, rating, and index

Range	**Rating**	**Index DRASTIC (ArAw)**	**Index SI (ArAw)**	**Area (%)**
Gravel	8	24	20.72	7.21
Conglomerate	6	18	15.54	83.42
Clay	4	12	5.18	9.38

Soil media

It is the upper part of the unsaturated zone characterized by biological activity, which influences the net recharge, which infiltrates into the aquifer, and has the capacity of a pollutant to travel until the groundwater (Aller *et al.* 1987; Anane *et al.* 2013b). Attenuation character of the soil media depends on the structure and the type of pollutants and the soil texture (Al Hallaq & Elaish 2012; Kumar *et al.* 2014). Besides, the attenuation process of filtration, sorption, volatilization, and biodegradation may be quite significant, where the soil is fairly thick (Aller *et al.* 1987; Bhuvaneswaran & Ganesh 2019). Soil texture spatial data were obtained from the soil map of 'la Carte Agricole' of Bouira department (spatial data source). To calculate the soil media index ratings, and the weight of 2, are used (Table 7). There are 3 classes of soil present in the plain.

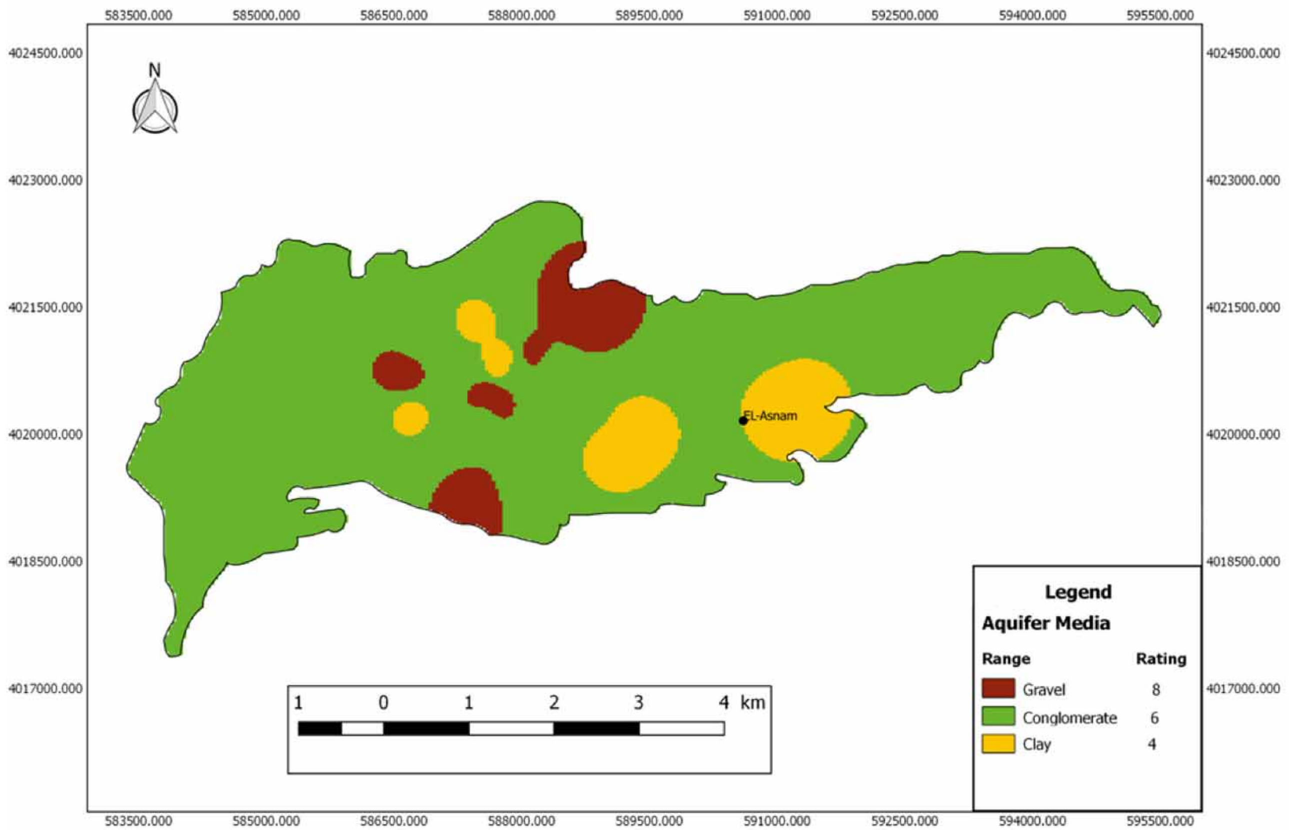

Figure 6 | Aquifer media map of El Asnam plain.

Table 7 | Soil media range, rating, and index

Range	Rating	Index (SrSw)	Area (%)
Gravelly sand	10	20	0.26
Clayey gravel	7	14	3.99
Clayey loam, clay	3	6	95.74

Clayey loam and clayey soil is the dominant textural type that represents 95.74% of the plain, clayey gravel soil 3.99%, and gravelly sand soil 0.26% at some places as shown in Figure 7.

Topography

It is represented by the slope and the slope variability of the land surface. Areas with low slopes allow retention of runoff water for longer times, which contributes to increasing the infiltration into the sub-surface (Fernandes *et al.* 2014), thus are more susceptible to groundwater pollution and vice versa (Rahman 2008). In this study, the surface slope has been generated from ASTER DEM. Categorized into three classes. The slope varies between 2 and 6% (very gentle slope) are located towards the south side, 6–12% (gentle slope) covers most of the study area (84.08%) conferring vulnerability to pollution, and 12–18% (moderate slope) are detected in the east side of the plain (Figure 8). Topography ratings weight and index according to standard DRASTIC are given in Table 8.

The impact of vadose zone

The vadose zone is the portion of terrain lying between the ground surface and the groundwater that can be discontinuously saturated or absolutely unsaturated (Kabera & Zhaohui 2008). It has an impact on the aquifer contamination and is alike to

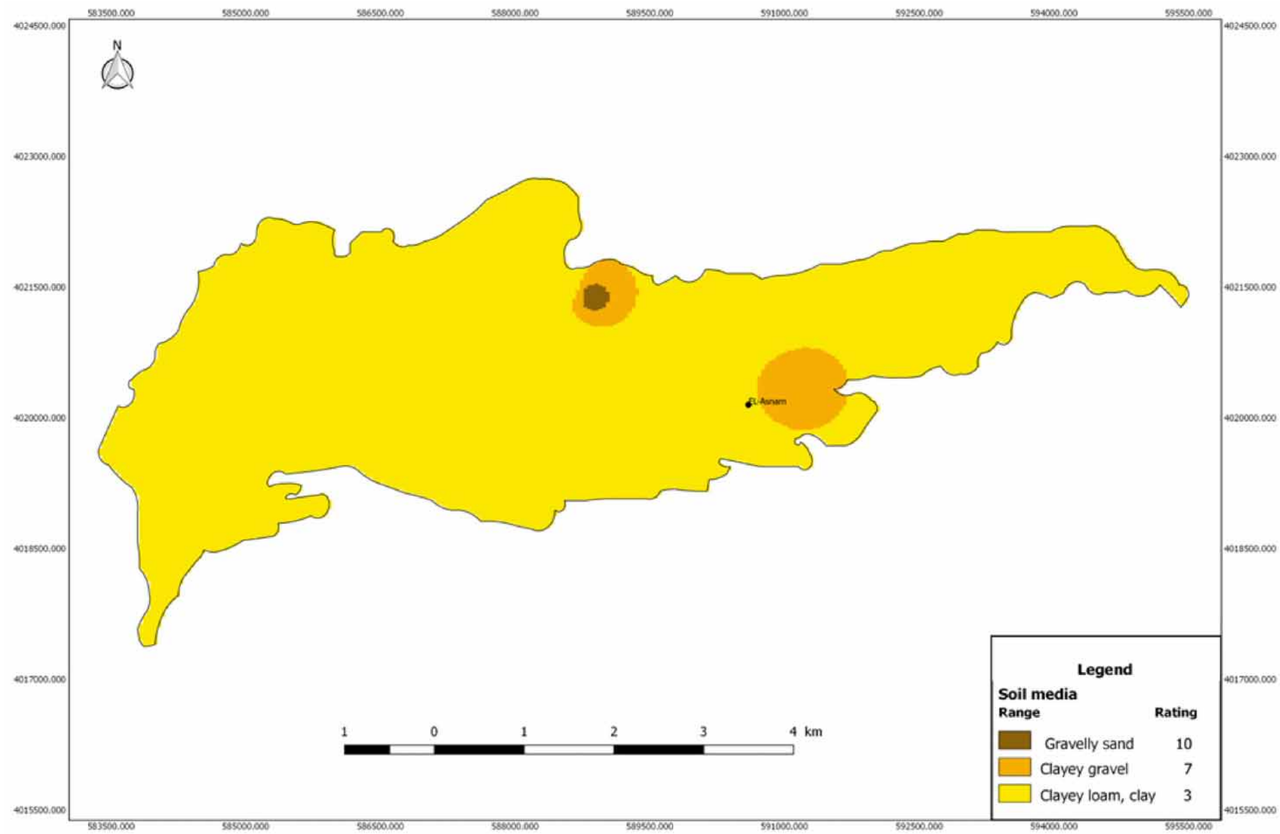

Figure 7 | Soil media map of El Asnam plain.

soil cover, depending on the attenuation characteristics of the media and on its permeability (Al Hallaq & Elaish 2012; Zghibi *et al.* 2016). Also, the type of vadose zone media identifies the characteristics of contamination attenuation such as sorption, filtration, biodegradation, dispersion, and volatilization (Aller *et al.* 1987). This parameter has been determined from the lithological logs of 20 boreholes in the plain. The vadose zone media comprises clay, clay with gravel, and sandstone. Two ranges are obtained according to Table 9, varying between 1 and 6. The map of this parameter is presented in Figure 9.

Hydraulic conductivity

It is the capacity of the materials of the aquifer to transmit water (Saha & Alam 2014; Machdar *et al.* 2018; Jhariya *et al.* 2019). This parameter polices the rate at which groundwater flows and eventually the rate of contaminant movement (Aller *et al.* 1987). When it is high, dispersion of pollutants in the aquifer increases, and the vulnerability is considered high (Chenini *et al.* 2015). In this study, the values of hydraulic conductivity were determinated from the transmissibility of the pumping tests of existing wells. Northern part of the plain (59.03%) shows high hydraulic conductivity, more than $9.4\ 10^{-4}$ m/s, with a rating of 10 (Table 10). 35.43% of the plain, located in the south part has moderate hydraulic conductivity varies from $3.29\ 10^{-4}$ to $4.7\ 10^{-4}$ m/s and a rating of 6. Low conductivity is distributed through small areas (4.79 and 0.75%) and assigned ratings 4 and 2 as indicated in the DRASTIC rating. The resulting map is presented in Figure 10.

Land use

The land use map presented four categories (Figure 11), two of which regard agricultural activities. Three ratings are obtained 0, 70, and 90 (Table 11). The rating of 90 is attributed to the vegetable crops and the cereals since these areas have an important influence on the infiltration of pollutants by recharging the aquifer, pertained to 79.78% of the plain. The rating of 70 corresponds to discontinuous urban areas, distributed throughout El Asnam plain, occupying 11.18% of the plain. The low rating of 0 was attributed to the forests that can be found in the east and the south of the plain with 9.04%, which are considered non-polluted.

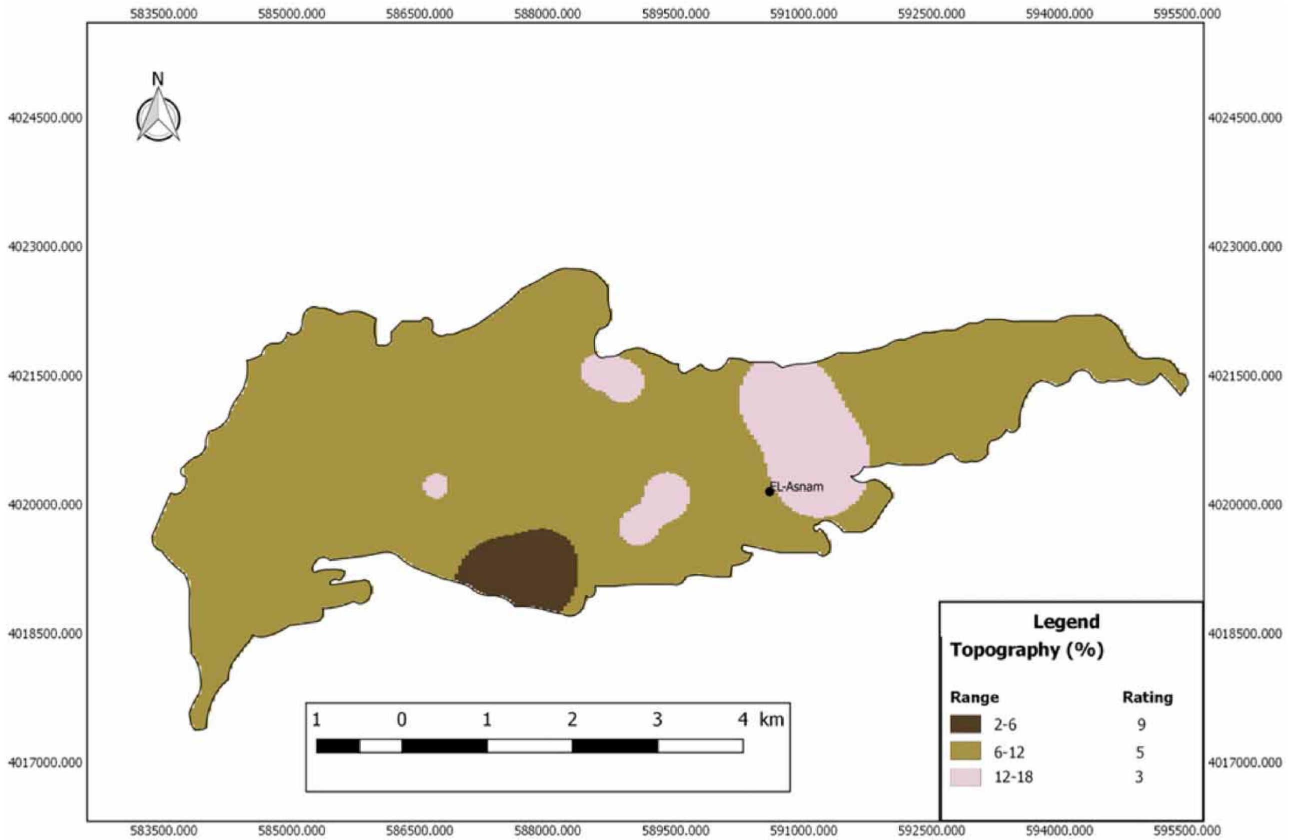

Figure 8 | Topography map of El Asnam plain.

Table 8 | Topography range, rating, and index

Range (%)	Rating	Index DRASTIC (Tr Tw)	Index SI (Tr Tw)	Area (%)
2–6	9	9	10.89	3.67
6–12	5	5	6.05	86.29
12–18	3	3	3.63	10.04

Table 9 | Impact of the vadose zone range, rating, and index

Range	Rating	Index (Irlw)	Area (%)
Clay	1	5	64.41
Clay and gravel, sandstone	6	30	35.59

DRASTIC vulnerability map

The DRASTIC index of the study area has been calculated by integrating 7 hydrogeological data layers with the GIS environment. It determines the groundwater susceptibiliy to pollution in the plain. The index values range between 103 and 176. The vulnerability of El Asnam plain was categorized into three classes such as low (77–104), moderate (104–130), and high (130–156). Table 12 presents the areas covered by each category. Figure 12 shows that 3.19% of the plain is exposed to low pollution and found in the south-central part, 90.13% is exposed as having moderate pollution potential in most of the plain, and, finally, 6.68% located in the central and eastern part have a high pollution potential. These results are identified in

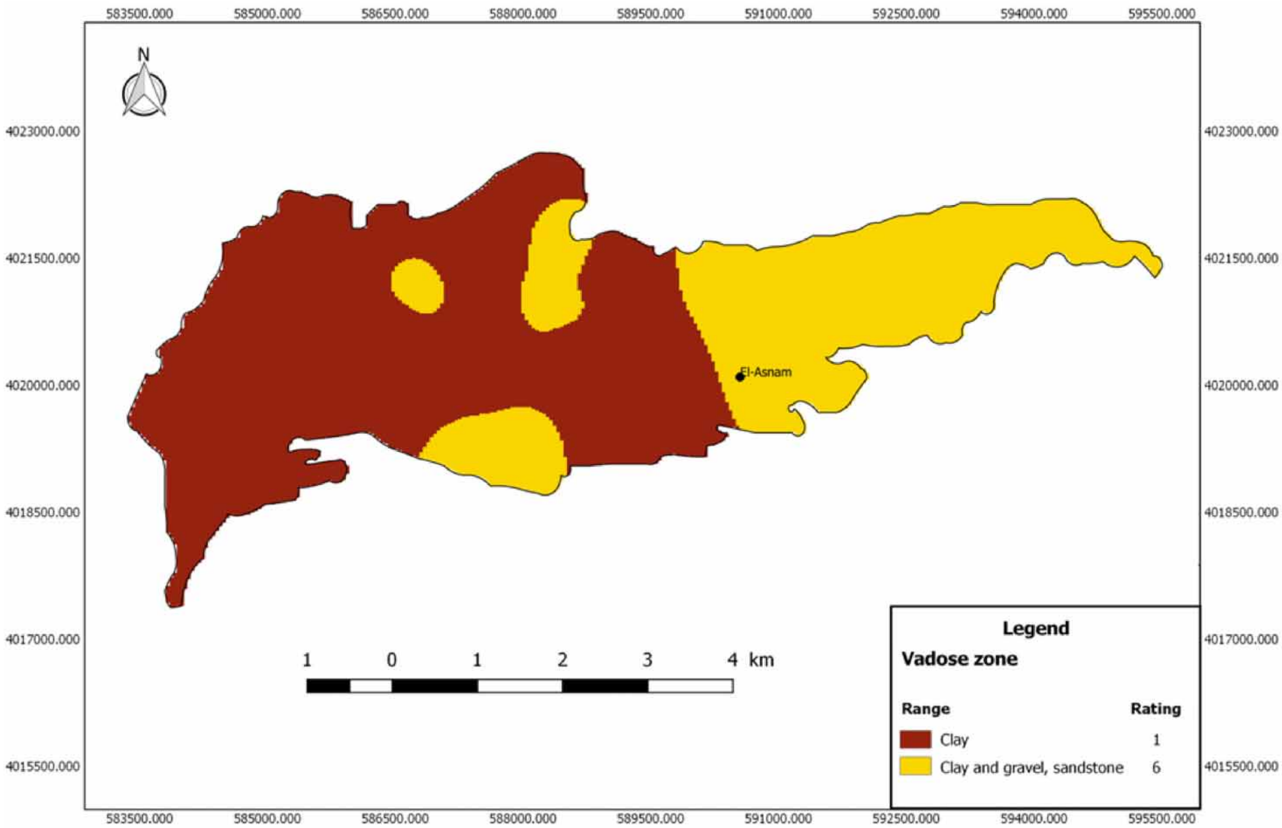

Figure 9 | Vadose zone map of El Asnam plain.

Table 10 | Hydraulic conductivity range, rating, and index

Range 10^{-4} (m/s)	Rating	Index (CrCw)	Area (%)
>9,4	10	30	59,03
3,29–4,7	6	18	35,43
1,47–3,29	4	12	4,79
0,47–1,47	2	6	0,75

the part of the plain with high scores of aquifer media, depth to the water table, hydraulic conductivity, and impact of the vadose zone, which are responsible for the high groundwater vulnerability, including domestic wastewater discharge of El Asnam city and poultry production units existing around the city. Particular attention must be required in these areas for any future decisions. However, the low vulnerability zone in the south-central part is due to the combination of all parameters except for the hydraulic conductivity. Moderately vulnerable zones are distributed in most of the plain due to the net recharge.

SI vulnerability map

The map of SI method was acquired after the calculation of the SI index. There are two types of vulnerability in El Asnam plain according to the SI method, high and moderate (Figure 13). The index values range from 49.73 to 79.97 as presented in Table 13. Most of the plain is classified as highly vulnerable (92.3%) to pollution. This result is mainly due to the continuous irrigation of vegetation crops and cereals and also caused by the overutilization of fertilizers and pesticides. Whereas 7.7% of the area, representing moderate vulnerability to contamination, is mostly located in the northeast and south of the study area, coinciding with the urban and forest areas, which explains this low rate.

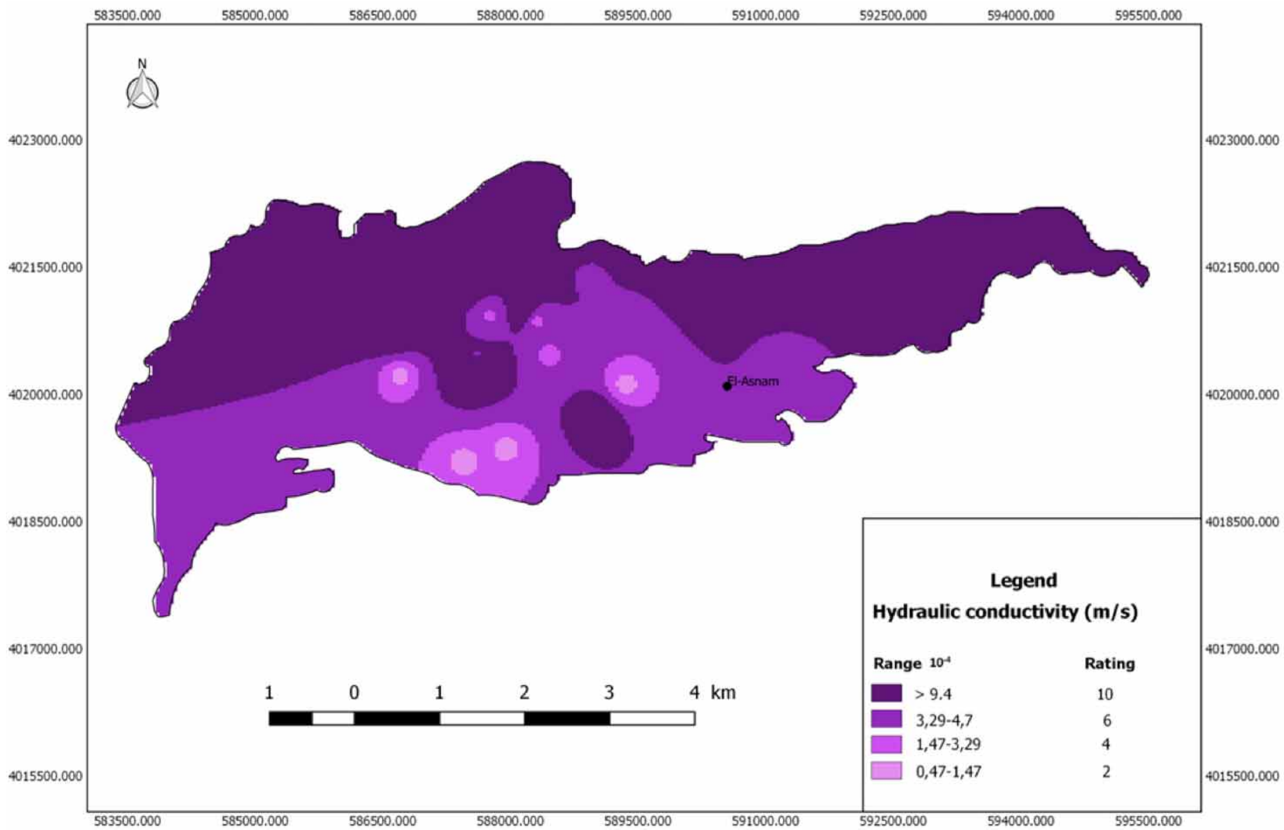

Figure 10 | Hydraulic conductivity map of El Asnam plain.

Validation of the vulnerability maps

To approve the vulnerability maps, it is very important to validate the DRASTIC and the SI models on El Asnam plain to pollution by considering the distribution of the nitrate values and the vulnerability categories of each method on the study area. Nitrate is a typical indicator of pollution caused mainly by anthropogenic activities (Jhariya 2019; Amiri *et al.* 2020a, 2020b). Agriculture is the main activity that requires the use of pesticides, thus allowing the leaching of nitrates by water infiltration represented by the parameter of net recharge (Feola *et al.* 2015). The 20 nitrate concentrations are collected in the wet period of 2016 were classified into three categories: <30 mg/l, 30–45 mg/l, >45 mg/l (limit of WHO). The correlation of these values and the classes of DRASTIC and SI models are presented in Figures 14 and 15.

By comparing the results of each method, it can be observed that 10 samples out of 20 have concentrations of nitrate exceeding 45 mg/l, correspond to the high class of the vulnerability of the SI method, reflecting a result of 50%. On the other hand, the validation of the DRASTIC method presents 35% of the results, only 7 vulnerability classes of the DRASTIC method coincide with the nitrate concentrations of these samples. The distribution of the concentrations of nitrate and the SI method have a correlation for half of the cases, which is the most appropriate method to evaluate groundwater vulnerability to pollution.

In this study, the SI method gives satisfactory results such as that of Anane *et al.* (2013b), Ayed *et al.* (2017), and Ncibi *et al.* (2020). According to these results, agricultural activities contributed to nitrate pollution of the groundwater of El Asnam plain.

CONCLUSION

Groundwater resources are a major source of domestic consumption and irrigation in El Asnam plain, located in Bouira region (Algeria). This area is characterized by agricultural lands, marked by excessive use of pesticides, which can induce a risk of groundwater pollution.

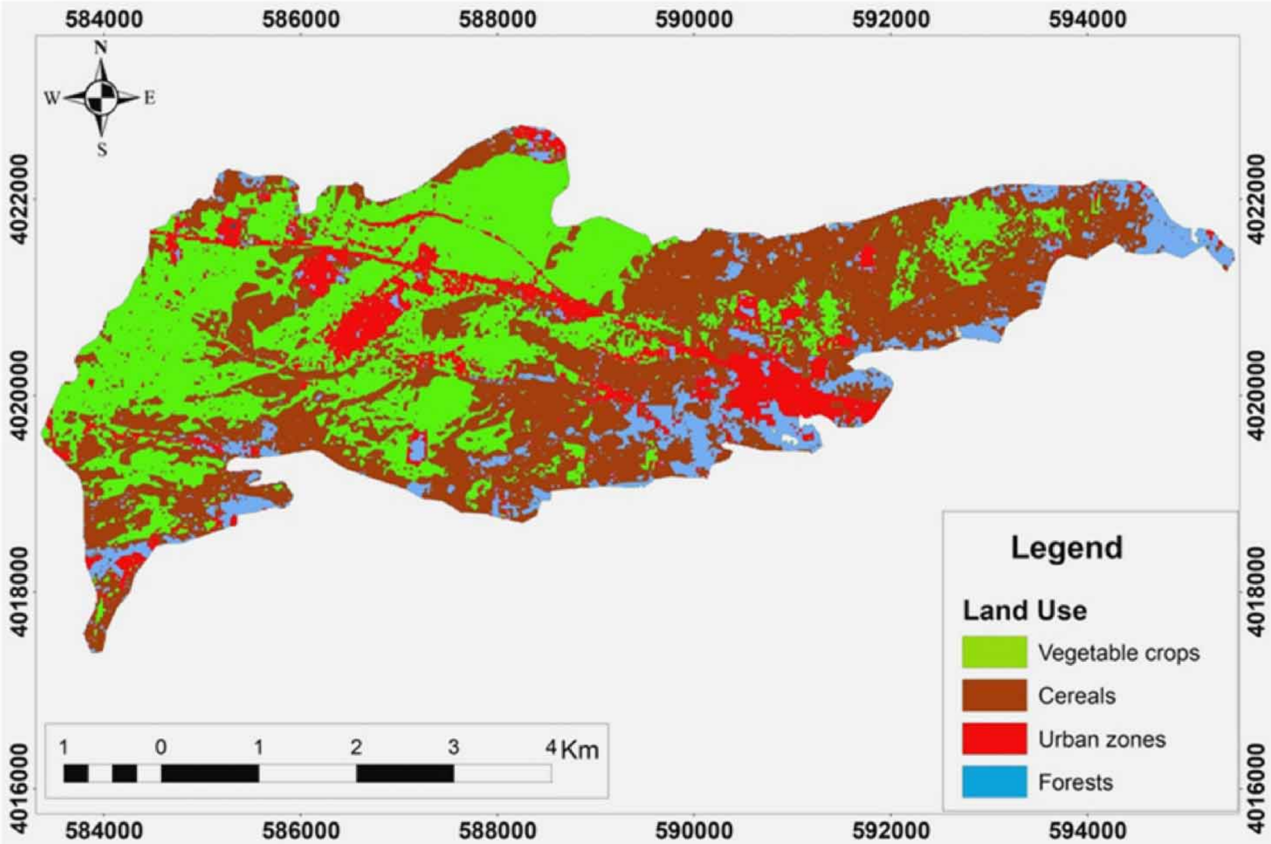

Figure 11 | Land use map of El Asnam plain.

Table 11 | Land use range, rating, and index

Land use	Rating	Index (Lu)	Area(%)
Vegetable crops and cereals	90	19.98	79.78
Urban zone	70	15.54	11,18
Forests	0	0	9,04

Table 12 | DRASTIC groundwater vulnerability zone distribution

DRASTIC index value	Area (%)	Vulnerability zone
77–104	3.19	Low
104–130	90.13	Moderate
130–156	6.68	High

An attempt to evaluate groundwater vulnerability to pollution in El Asnam plain has been carried out in this study. This task was conducted using the DRASTIC and the SI models in a GIS environment. The DRASTIC model includes 7 parameters to present the hydrogeological characteristics of the aquifer, i.e., depth to water level, net recharge, aquifer media,

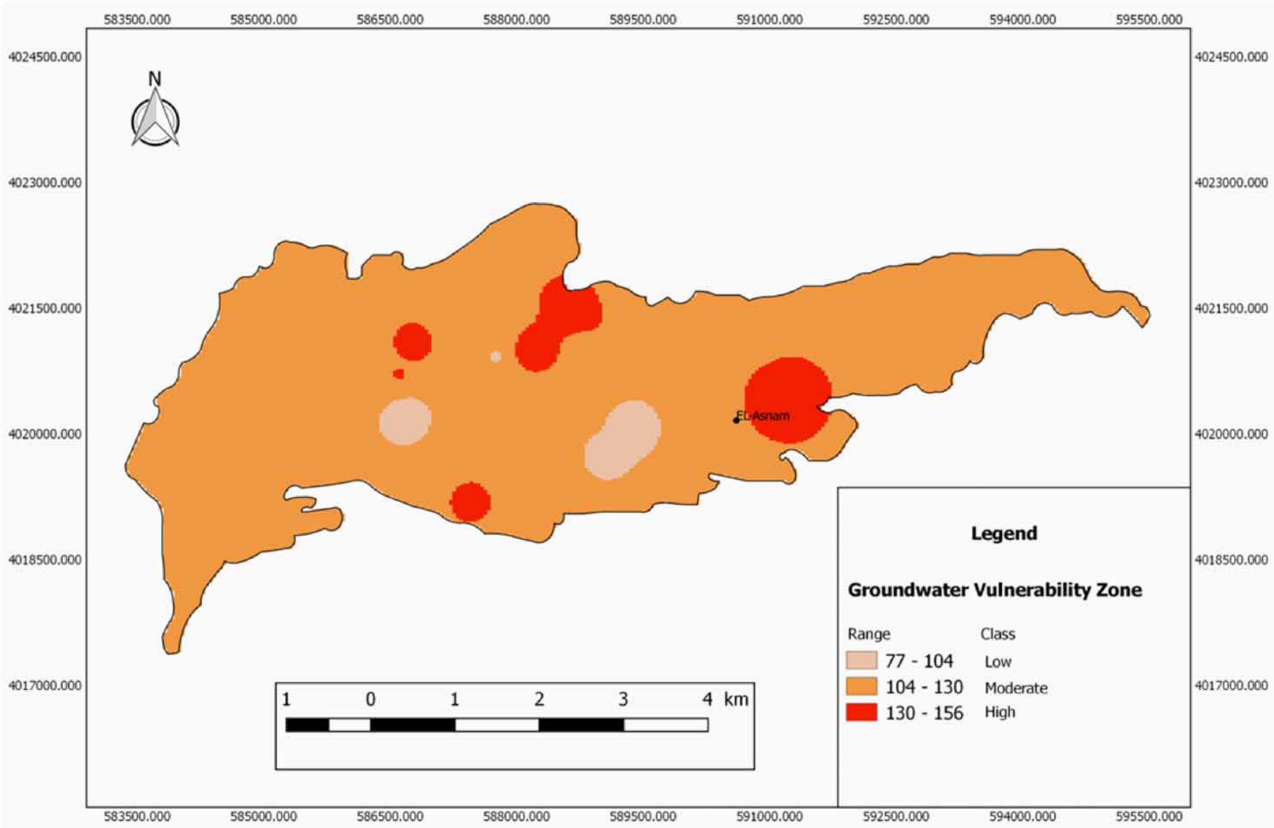

Figure 12 | DRASTIC groundwater vulnerability map of El Asnam plain.

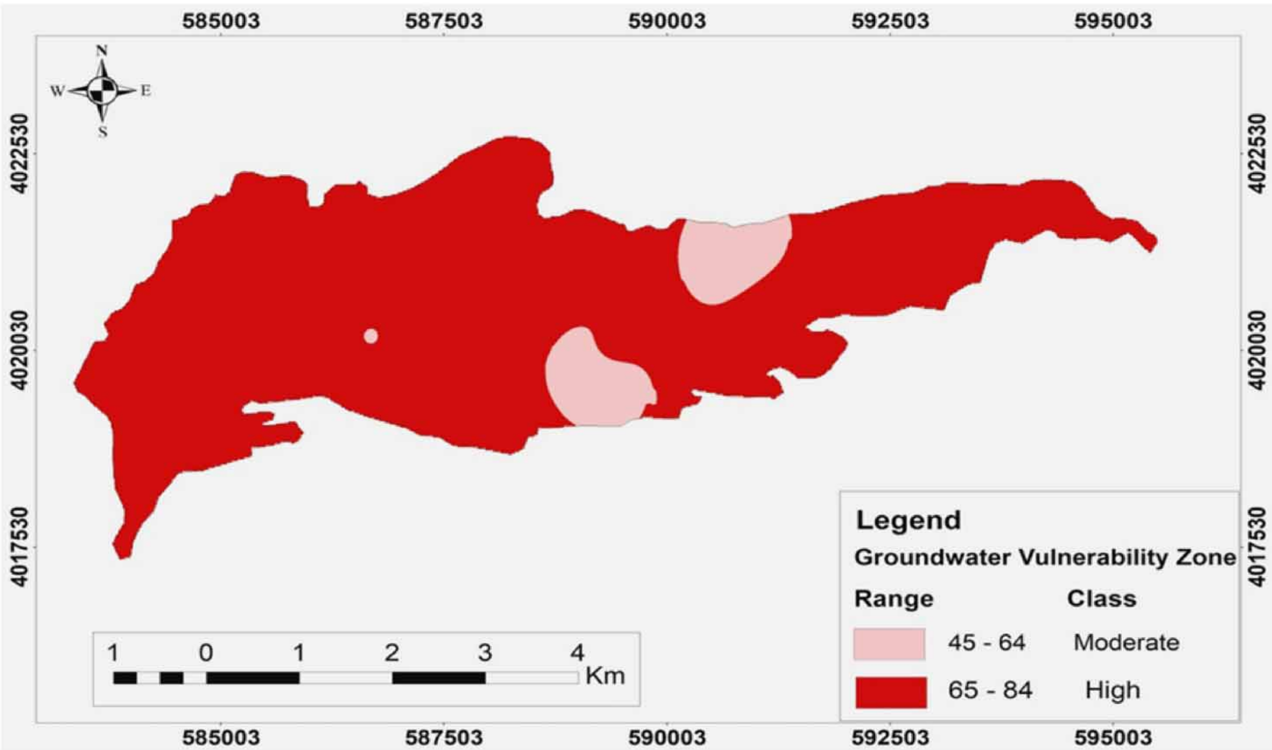

Figure 13 | SI groundwater vulnerability map of El Asnam plain.

Table 13 | SI groundwater vulnerability zone distribution

SI index value	Area (%)	Vulnerability zone
45–64	7,7	Moderate
65–84	92,3	High

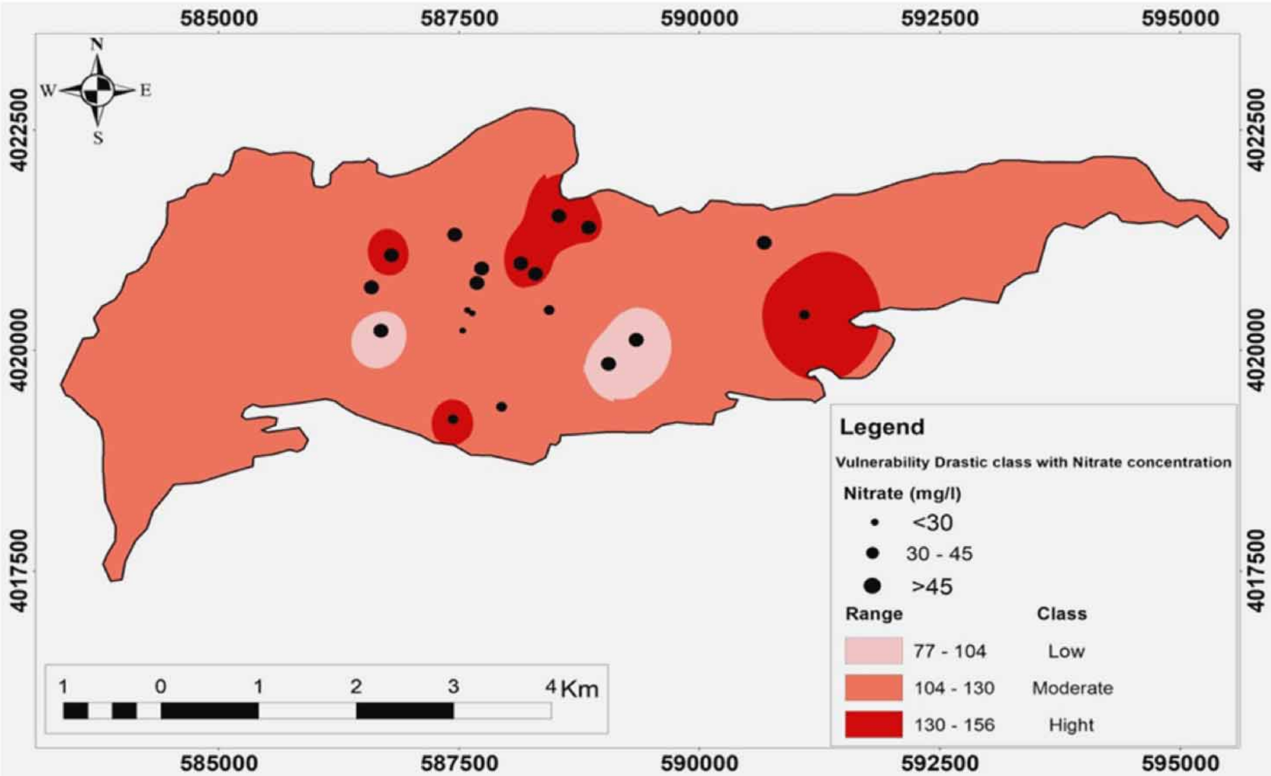

Figure 14 | Correlation of DRASTIC vulnerability classes and nitrate concentrations.

soil media, topography, the impact of the vadose zone, and hydraulic conductivity. Parameters data was incorporated in GIS for obtaining the map of the groundwater vulnerability.

In accordance with the DRASTIC index, the vulnerable areas were categorized into 3 zones with high, moderate, and low values, which cover 6.68, 90.13, and 3.19% of the plain respectively. It could be observed that the central and eastern part of the plain was a high vulnerability potential to pollution that originates from the shallow depth of water table, high scores of aquifer media, hydraulic conductivity, and impact of the vadose zone.

However, SI is a vulnerability model based on 5 parameters; 4 of them are the same as the DRASTIC method (depth to the water table, net recharge, aquifer media, and topography); the last one is the land use allowing to represent anthropogenic activities on the ground surface. However, the SI vulnerability map shows that the high vulnerability category covers 92.3% of the area the rest was found moderately vulnerable (7.7%). These results can be explained by the high recharge, the low topography, and the intense agricultural activities' impact.

To compare the application of these methods, validation to the repartition of the nitrate concentrations throught the plain was essential. The results indicate that the coincidence between the classes of vulnerability and the repartition of the nitrate concentrations values of the DRASTIC and SI methods are 35 and 50% respectively.

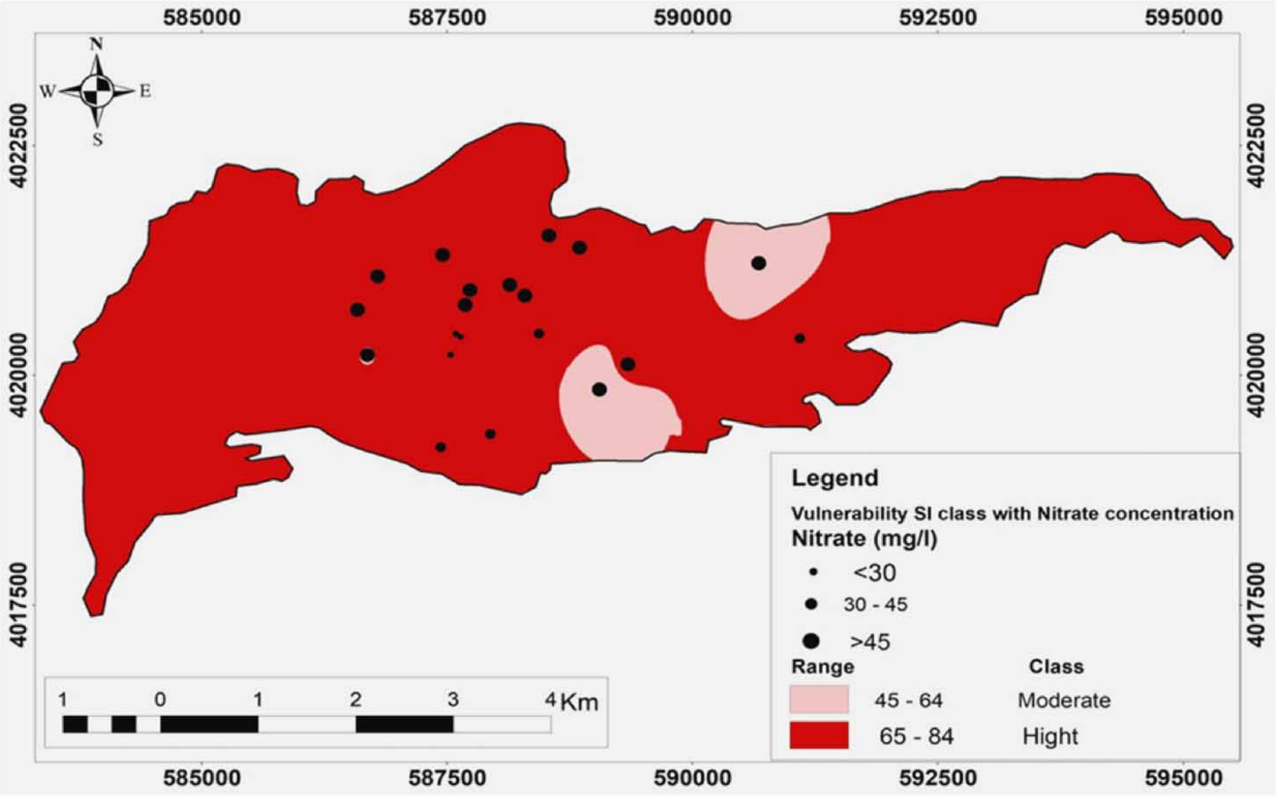

Figure 15 | Correlation of SI vulnerability classes and nitrate concentrations.

The SI method compared to the DRASTIC method shows a satisfactory correlation with the nitrate concentrations values, thus showing that the NO_3^- has the biggest influence in the plain because of the land use parameter that introduces the effect of the overuse of fertilizers in the agricultural areas.

Finally, this study also offers an economical tool for the groundwater resources responsibles, as it gives an efficient assessment of groundwater vulnerability mainly caused by agricultural activities.

DATA AVAILABILITY STATEMENT

All relevant data are included in the paper or its Supplementary Information.

REFERENCES

Abdeslam, I., Fehdi, C. & Djabri, L. 2017 Application of drastic method for determining the vulnerability of an alluvial aquifer: Morsott-El Aouinet north east of Algeria: using arcgis environment. *Energy Procedia* **119**, 308–317.

Abdullahi, U. S. 2009 Evaluation of models for assessing groundwater vulnerability to pollution in Nigeria. *Bayero Journal of Pure and Applied Sciences* **2**, 138–142.

Ahirwar, S. & Shukla, J. P. 2018 Assessment of groundwater vulnerability in Upper Betwa River Watershed using GIS based DRASTIC model. *Journal of the Geological Society of India* **91**, 334–340.

Al Hallaq, A. H. & Elaish, B. S. A. 2012 Assessment of aquifer vulnerability to contamination in Khanyounis Governorate, Gaza Strip – Palestine, using the DRASTIC model within GIS environment. *Arabian Journal of Geosciences* **5**, 833–847.

Aller, L., Bennett, T., Lehr, J., Petty, R. & Hackett, G. 1987 *DRASTIC: A Standardized System for Evaluating Ground Water Pollution Potential Using Hydrogeologic Settings*. US Environmental Protection Agency. Washington, DC, p. 455.

Almasri, M. N. 2008 Assessment of intrinsic vulnerability to contamination for Gaza coastal aquifer, Palestine. *Journal of Environmental Management* **88**, 577–593.

Al-Shatnawi, A. M., Al-Shboul, R., Al-Fawwaz, B. M., Al-Sharafat, W. & Khalf, R. M. B. 2014 Vulnerability assessment using raster calculation and DRASTIC model for the Jordan valley subsurface basin (AB1) imaging maps. *Journal of Geographic Information System* **6**, 585.

Amiri, F., Tabatabaie, T. & Entezari, M. 2020a GIS-based DRASTIC and modified DRASTIC techniques for assessing groundwater vulnerability to pollution in Torghabeh-Shandiz of Khorasan County, Iran. *Arabian Journal of Geosciences* **13**, 479.

Amiri, F., Tabatabaie, T. & Entezari, M. 2020b GIS-based DRASTIC and modified DRASTIC techniques for assessing groundwater vulnerability to pollution in Torghabeh-Shandiz of Khorasan County, Iran. *Arabian Journal of Geosciences* **13**, 1–16.

Anane, M., Abidi, B., Lachaal, F., Limam, A. & Jellali, S. 2013a *DRASTIC-SIG, DRASTIC Pesticide et Indice de Sensibilité (SI): étude comparative pour l'évaluation de la pollution potentielle de l'aquifère superficiel de Nabeul-Hammamet, Tunisie Los modelos DRASTIC, DRASTIC pesticidas y el índice de susceptibilidad (SI) con base en SIG: estudio comparativo para la evaluación de la contaminación potencial del acuífero somero de Nabeul-Hammamet, Túnez* مؤشرات" دراستك" و" دراستك-مبيد" و" اسآ" باستخدام نظم المعلومات الجغرافية. دراسة مقارنة لتقييم امكانية تلوث المائدة المائية السطحية نابل-حمامات بتونس 基于 *GIS* 的 *DRASTIC* 模型*, Pesticide DRASTIC* 模型和敏感性指数 *(SI)* 模型*:* 关于突尼斯 *Nabeul-Hammamet* 浅部含水层潜在污染评估的对比研究 *Índices DRASTIC, DRASTIC Pesticida e Índice de Suscetibilidade (IS) com suporte de SIG: estudo comparativo para avaliação da poluição potencial no aquífero pouco profundo de Nabeul-Hammamet, Tunísia*.

Anane, M., Abidi, B., Lachaal, F., Limam, A. & Jellali, S. 2013b GIS-based DRASTIC, pesticide DRASTIC and the susceptibility index (SI): comparative study for evaluation of pollution potential in the Nabeul-Hammamet shallow aquifer, Tunisia. *Hydrogeology Journal* **21**, 715–731.

Anwar, M., Prem, C. & Rao, V. 2002 Evaluation of groundwater potential of Musi River catchment using DRASTIC index model, Hydrology and watershed management. In *Proceedings of the International Conference*, pp. 18–20.

Awawdeh, M., Obeidat, M. & Zaiter, G. 2015 Groundwater vulnerability assessment in the vicinity of Ramtha wastewater treatment plant, North Jordan. *Applied Water Science* **5**, 321–334.

Aydi, W., Saidi, S., Chalbaoui, M., Chaibi, S. & Dhia, H. B. 2013 Evaluation of the groundwater vulnerability to pollution using an intrinsic and a specific method in a GIS environment: application to the Plain of Sidi Bouzid (Central Tunisia). *Arabian Journal for Science and Engineering* **38**, 1815–1831.

Ayed, B., Jmal, I., Sahal, S. & Bouri, S. 2017 Assessment of groundwater vulnerability using a specific vulnerability method: case of Maritime Djeffara shallow aquifer (Southeastern Tunisia). *Arabian Journal of Geosciences* **10**, 262.

Baalousha, H. 2006 Vulnerability assessment for the Gaza Strip, Palestine using DRASTIC. *Environmental Geology* **50**, 405–414.

Babiker, I. S., Mohamed, M. A., Hiyama, T. & Kato, K. 2005 A GIS-based DRASTIC model for assessing aquifer vulnerability in Kakamigahara Heights, Gifu Prefecture, central Japan. *Science of the Total Environment* **345**, 127–140.

Barbulescu, A. 2020 Assessing groundwater vulnerability: DRASTIC and DRASTIC-like methods: a review. *Water* **12**, 1356.

Bera, A., Mukhopadhyay, B. P., Chowdhury, P., Ghosh, A. & Biswas, S. 2021 Groundwater vulnerability assessment using GIS-based DRASTIC model in Nangasai River Basin, India with special emphasis on agricultural contamination. *Ecotoxicology and Environmental Safety* **214**, 112085.

Bhuvaneswaran, C. & Ganesh, A. 2019 Spatial assessment of groundwater vulnerability using DRASTIC model with GIS in Uppar odai sub-watershed, Nandiyar, Cauvery Basin, Tamil Nadu. *Groundwater for Sustainable Development* **9**, 100270.

Boumaiza, L., Walter, J., Chesnaux, R., Brindha, K., Elango, L., Rouleau, A., Wachniew, P. & Stumpp, C. 2021 An operational methodology for determining relevant DRASTIC factors and their relative weights in the assessment of aquifer vulnerability to contamination. *Environmental Earth Sciences* **80**, 1–19.

Chenini, I., Zghibi, A. & Kouzana, L. 2015 Hydrogeological investigations and groundwater vulnerability assessment and mapping for groundwater resource protection and management: state of the art and a case study. *Journal of African Earth Sciences* **109**, 11–26.

Chitsazan, M. & Akhtari, Y. 2009 A GIS-based DRASTIC model for assessing aquifer vulnerability in Kherran Plain, Khuzestan, Iran. *Water Resources Management* **23**, 1137–1155.

Europea, C. 1993 *CORINE Land Cover Guide Technique*. Office des Pubblications Officielles des Communautés Européennes, Luxembourg.

Feola, G., Lerner, A. M., Jain, M., Montefrio, M. J. F. & Nicholas, K. A. 2015 Researching farmer behaviour in climate change adaptation and sustainable agriculture: lessons learned from five case studies. *Journal of Rural Studies* **39**, 74–84.

Fernandes, L. F. S., Cardoso, L. V. R. Q., Pacheco, F. A. L., Leitão, S. & Moura, J. P. 2014 DRASTIC and GOD vulnerability maps of the Cabril River Basin, Portugal. *Rem: Revista Escola de Minas* **67**, 133–142.

Francés, A., Paralta, E., Fernandes, J. & Ribeiro, L. 2001 Development and application in the Alentejo region of a method to assess the vulnerability of groundwater to diffuse agricultural pollution: the susceptibility index. In: *3rd International Conference on Future Groundwater Resources at Risk*, IAH/Unesco.

Ghazavi, R. & Ebrahimi, Z. 2015 Assessing groundwater vulnerability to contamination in an arid environment using DRASTIC and GOD models. *International Journal of Environmental Science and Technology* **12**, 2909–2918.

Hasan, M., Islam, A., Hasan, M. A., Alam, J. & Peas, M. H. 2019 Groundwater vulnerability assessment in Savar upazila of Dhaka district, Bangladesh – a GIS-based DRASTIC modeling. *Groundwater for Sustainable Development* **9**, 100220.

Hrkal, Z. 2001 Vulnerability of groundwater to acid deposition, Jizerske Mountains, northern Czech Republic: construction and reliability of a GIS-based vulnerability map. *Hydrogeology Journal* **9**, 348–357.

Huan, H., Wang, J. & Teng, Y. 2012 Assessment and validation of groundwater vulnerability to nitrate based on a modified DRASTIC model: a case study in Jilin City of northeast China. *Science of The Total Environment* **440**, 14–23.

Iqbal, J., Pathak, G. & Gorai, A. K. 2015 Development of hierarchical fuzzy model for groundwater vulnerability to pollution assessment. *Arabian Journal of Geosciences* **8**, 2713–2728.

Jamrah, A., Al-Futaisi, A., Rajmohan, N. & Al-Yaroubi, S. 2008 Assessment of groundwater vulnerability in the coastal region of Oman using DRASTIC index method in GIS environment. *Environmental Monitoring and Assessment* **147**, 125–138.

Jhariya, D. C. 2019 Assessment of groundwater pollution vulnerability using GIS-based DRASTIC model and its validation using nitrate concentration in Tandula Watershed, Chhattisgarh. *Journal of the Geological Society of India* **93**, 567–573.

Jhariya, D. C., Kumar, T., Pandey, H. K., Kumar, S., Kumar, D., Gautam, A. K., Baghel, V. S. & Kishore, N. 2019 Assessment of groundwater vulnerability to pollution by modified DRASTIC model and analytic hierarchy process. *Environmental Earth Sciences* **78**, 610.

Jilali, A., Zarhloule, Y. & Georgiadis, M. 2015 Vulnerability mapping and risk of groundwater of the oasis of Figuig, Morocco: application of DRASTIC and AVI methods. *Arabian Journal of Geosciences* **8**, 1611–1621.

Kabera, T. & Zhaohui, L. 2008 A GIS based DRASTIC model for assessing groundwater in shallow aquifer in Yuncheng Basin, Shanxi, China. *Research Journal of Applied Sciences* **3**, 195–205.

Kadkhodaie, F., Asghari Moghaddam, A., Barzegar, R., Gharekhani, M. & Kadkhodaie, A. 2019 Optimizing the DRASTIC vulnerability approach to overcome the subjectivity: a case study from Shabestar plain, Iran. *Arabian Journal of Geosciences* **12**, 527.

Khan, R. & Jhariya, D. C. 2019 Assessment of groundwater pollution vulnerability using GIS based modified DRASTIC model in Raipur City, Chhattisgarh. *Journal of the Geological Society of India* **93**, 293–304.

Kumar, S., Thirumalaivasan, D. & Radhakrishnan, N. 2014 GIS based assessment of groundwater vulnerability using drastic model. *Arabian Journal for Science and Engineering* **39**, 207–216.

Lake, I. R., Lovett, A. A., Hiscock, K. M., Betson, M., Foley, A., Sünnenberg, G., Evers, S. & Fletcher, S. 2003 Evaluating factors influencing groundwater vulnerability to nitrate pollution: developing the potential of GIS. *Journal of Environmental Management* **68**, 315–328.

Machdar, I., Zulfikar, T., Rinaldi, W. & Alfiansyah, Y. 2018 Assessment of groundwater vulnerability using DRASTIC Model and GIS: a case study of two sub-districts in Banda Aceh city, Indonesia. In: *IOP Conference Series: Materials Science and Engineering*, IOP Publishing, p. 012032.

Magesh, N. S. & Chandrasekar, N. 2013 Evaluation of spatial variations in groundwater quality by WQI and GIS technique: a case study of Virudunagar District, Tamil Nadu, India. *Arabian Journal of Geosciences* **6**, 1883–1898.

Mallik, S., Bhowmik, T., Mishra, U. & Paul, N. 2021 Local scale groundwater vulnerability assessment with an improved DRASTIC model. *Natural Resources Research* **30**, 2145–2160.

Mondal, I., Bandyopadhyay, J. & Chowdhury, P. 2019 A GIS based DRASTIC model for assessing groundwater vulnerability in Jangalmahal area, West Bengal, India. *Sustainable Water Resources Management* **5**, 557–573.

Muhammad, A. M., Zhonghua, T., Dawood, A. S. & Earl, B. 2015 Evaluation of local groundwater vulnerability based on DRASTIC index method in Lahore, Pakistan. *Geofísica Internacional* **54**, 67–81.

Nadiri, A. A., Sedghi, Z., Khatibi, R. & Sadeghfam, S. 2018 Mapping specific vulnerability of multiple confined and unconfined aquifers by using artificial intelligence to learn from multiple DRASTIC frameworks. *Journal of Environmental Management* **227**, 415–428.

Nadiri, A. A., Norouzi, H., Khatibi, R. & Gharekhani, M. 2019 Groundwater DRASTIC vulnerability mapping by unsupervised and supervised techniques using a modelling strategy in two levels. *Journal of Hydrology* **574**, 744–759.

Narmada, K., Bhaskaran, G. & Gobinath, K. 2015 Assessment of groundwater quality in the Amaravathi River Basin, South India. In: *Environmental Management of River Basin Ecosystems*. In: Ramkumar, M., Kumaraswamy, K., Mohanraj, R. (eds) Environmental Management of River Basin Ecosystems. Springer Earth System Sciences. Springer, Cham, 549–573.

Ncibi, K., Chaar, H., Hadji, R., Baccari, N., Sebei, A., Khelifi, F., Abbes, M. & Hamed, Y. 2020 A GIS-based statistical model for assessing groundwater susceptibility index in shallow aquifer in Central Tunisia (Sidi Bouzid basin). *Arabian Journal of Geosciences* **13**, 98.

Neh, A. V., Ako, A. A., Ayuk II, A. R. & Hosono, T. 2015 DRASTIC-GIS model for assessing vulnerability to pollution of the phreatic aquiferous formations in Douala–Cameroon. *Journal of African Earth Sciences* **102**, 180–190.

O.N.I.D. 1990 *Office National de l'irrigation et du drainage. Etude de l'amenagement hydro-agricole de la vallée de l'oued Sahel et du plateau d'El Asnam-rapport des analyses des ressources en eau et des ressources en sol.*

Oroji, B. & Karimi, Z. F. 2018 Application of DRASTIC model and GIS for evaluation of aquifer vulnerability: case study of Asadabad, Hamadan (western Iran). *Geosciences Journal* **22**, 843–855.

Pacheco, F., Pires, L., Santos, R. & Fernandes, L. S. 2015 Factor weighting in DRASTIC modeling. *Science of The Total Environment* **505**, 474–486.

Pathak, S., Gupta, S. & Ojha, C. 2021 Assessment of groundwater vulnerability to contamination with ASSIGN index: a case study in Haridwar, Uttarakhand, India. *Journal of Hazardous, Toxic, and Radioactive Waste* **25**, 04020081.

Rahman, A. 2008 A GIS based DRASTIC model for assessing groundwater vulnerability in shallow aquifer in Aligarh, India. *Applied Geography* **28**, 32–53.

Ramakrishna, B., Rajasekhar, P. & Vaheed, S. 2020 Assessment of aquifer vulnerability of Nizamabad District, Telangana State, India using GIS and drastic method. In: Satapathy, S., Raju, K., Molugaram, K., Krishnaiah, A., Tsihrintzis, G. (eds) International Conference on Emerging Trends in Engineering (ICETE). Learning and Analytics in Intelligent Systems, vol 2. Springer, Cham, pp. 18–26.

Ribeiro, L. 2000 *Desenvolvimento de um índice para avaliar a susceptibilidade dos aquíferos à contaminação. Nota interna,(não publicada)*. ERSHA-CVRM.

Ribeiro, L., Pindo, J. C. & Dominguez-Granda, L. 2017 Assessment of groundwater vulnerability in the Daule aquifer, Ecuador, using the susceptibility index method. *Science of The Total Environment* **574**, 1674–1683.

Saha, D. & Alam, F. 2014 Groundwater vulnerability assessment using DRASTIC and pesticide DRASTIC models in intense agriculture area of the Gangetic plains, India. *Environmental Monitoring and Assessment* **186**, 8741–8763.

Saidi, S., Bouri, S. & Ben Dhia, H. 2010 Groundwater vulnerability and risk mapping of the Hajeb-jelma aquifer (Central Tunisia) using a GIS-based DRASTIC model. *Environmental Earth Sciences* **59**, 1579–1588.

Sarkar, M. & Pal, S. C. 2021 Application of DRASTIC and modified DRASTIC models for modeling groundwater vulnerability of Malda District in West Bengal. *Journal of the Indian Society of Remote Sensing* **49**, 1201–1219.

Sener, E. & Davraz, A. 2013 Assessment of groundwater vulnerability based on a modified DRASTIC model, GIS and an analytic hierarchy process (AHP) method: the case of Egirdir Lake basin (Isparta, Turkey). *Hydrogeology Journal* **21**, 701–714.

Shekhar, S. & Pandey, A. 2015 A GIS-based DRASTIC model for assessing groundwater vulnerability in hard rock granitic aquifer. *Arabian Journal of Geosciences* **8**, 1385–1401.

Sinan, M. & Razack, M. 2009 An extension to the DRASTIC model to assess groundwater vulnerability to pollution: application to the Haouz aquifer of Marrakech (Morocco). *Environmental Geology* **57**, 349–363.

Srinivasamoorthy, K., Vijayaraghavan, K., Vasanthavigar, M., Sarma, S., Chidambaram, S., Anandhan, P. & Manivannan, R. 2012 Assessment of groundwater quality with special emphasis on fluoride contamination in crystalline bed rock aquifers of Mettur region, Tamilnadu, India. *Arabian Journal of Geosciences* **5**, 83–94.

Stigter, T., Ribeiro, L. & Dill, A. C. 2006 Evaluation of an intrinsic and a specific vulnerability assessment method in comparison with groundwater salinisation and nitrate contamination levels in two agricultural regions in the south of Portugal. *Hydrogeology Journal* **14**, 79–99.

Teng, Y., Zuo, R., Xiong, Y., Wu, J., Zhai, Y. & Su, J. 2019 Risk assessment framework for nitrate contamination in groundwater for regional management. *Science of The Total Environment* **697**, 134102.

van Beynen, P. E., Niedzielski, M., Bialkowska-Jelinska, E., Alsharif, K. & Matusick, J. 2012 Comparative study of specific groundwater vulnerability of a karst aquifer in central Florida. *Applied Geography* **32**, 868–877.

Venkatesan, G., Pitchaikani, S. & Saravanan, S. 2019 Assessment of groundwater vulnerability using GIS and DRASTIC for Upper Palar River Basin, Tamil Nadu. *Journal of the Geological Society of India* **94**, 387–394.

Williams, J. & Kissel, D. 1991 Water percolation: an indicator of nitrogen-leaching potential. In: Follet R. F., Keeney D. R., Cruse R. M., eds, Managing nitrogen for groundwater quality and farm profitability. Madison, Wisconsin: Soil Science Society of America, Inc.; 1991. p. 59–83.

Zghibi, A., Merzougui, A., Chenini, I., Ergaieg, K., Zouhri, L. & Tarhouni, J. 2016 Groundwater vulnerability analysis of Tunisian coastal aquifer: an application of DRASTIC index method in GIS environment. *Groundwater for Sustainable Development* **2**, 169–181.

Zhang, D., Huang, X.-Y. & Liu, Y.-T. 2010 Shallow groundwater vulnerability assessment in the Upper and Middle Reaches of the Huai River. In *2010 4th International Conference on Bioinformatics and Biomedical Engineering*, IEEE, pp. 1–3.

Zhao, Y. & Pei, Y. 2012 Risk evaluation of groundwater pollution by pesticides in China: a short review. *Procedia Environmental Sciences* **13**, 1739–1747.

First received 15 March 2022; accepted in revised form 16 May 2022. Available online 27 May 2022